Functional mapping of neurons in primary visual cortex using computational barcodes

neurotheory.umd.edu

Isabel Fernandez[1], Jan Antolik[2], Daniel A. Butts[3]

[1]Applied Mathematics & Statistics, and Scientific Computation Program, University of Maryland, [2]Faculty of Mathematics and Physics, KSVI, Charles University, Prague, Czech Republic,
[3]Program in Neuroscience and Cognitive Science, University of Maryland

UNIVERSITY OF MARYLAND

Introduction

Visual processing is performed over large neuronal populations distributed over many layers and areas. ***How is it possible to understand the role of individual neurons and circuits (and their specific physiological properties) in such global computation?*** Traditional approaches are based on characterizing one or a small set of "features" signaled by each neuron's response (e.g., [1]). Here, we explore an alternative: using **computational barcodes** to characterize the visual processing performed by each neuron in a shared functional space [2,3,4,5] derived using deep neural networks. Here we optimize and validate this approach using data generated by a dynamical simulation of V1 neurons with known circuits and architecture.

Single cell quadratic "energy model"

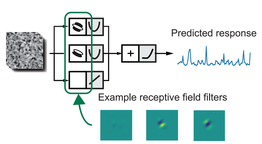

Population recodings

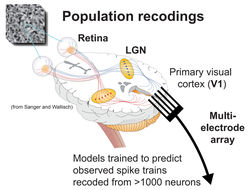

How do we interpret the role of individual neurons in global computations?

Population CNN-based model

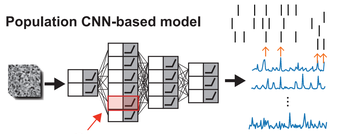

Computational barcodes

Neuron-specific readout weights across model depth show the composition of each neurons computation using a common "functional basis". [2,3,4,5]

Biologically constrained CNN architecture

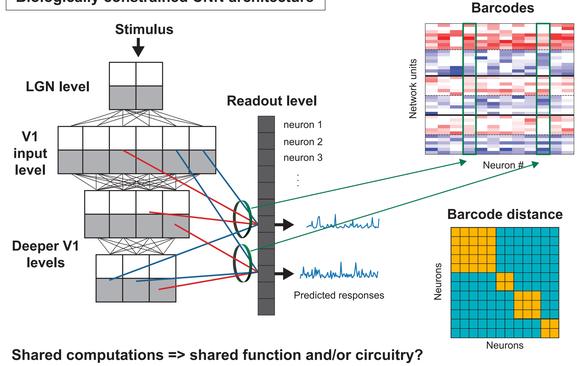

Shared computations => shared function and/or circuitry?

Interpretability via biological constraints

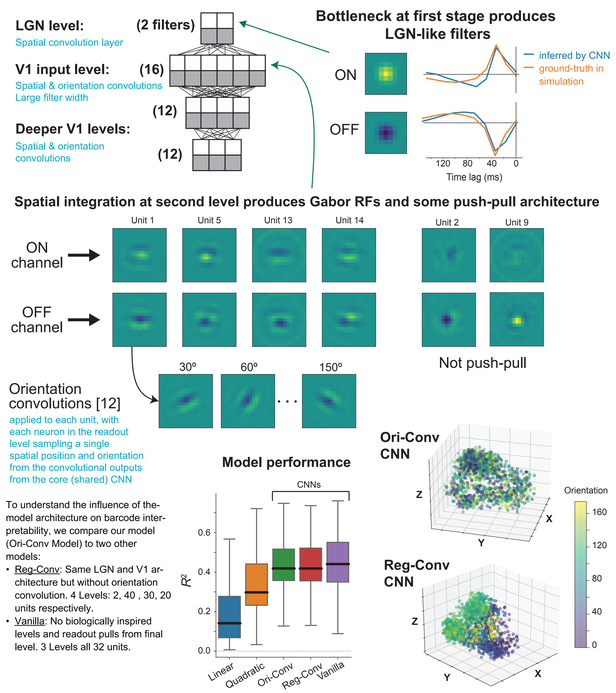

To understand the influence of the-model architecture on barcode interpretability, we compare our model (Ori-Conv Model) to two other models:

- Reg-Conv: Same LGN and V1 architecture but without orientation convolution. 4 Levels: 2, 40 , 30, 20 units respectively.
- Vanilla: No biologically inspired levels and readout pulls from final level. 3 Levels all 32 units.

Barcode metrics to identify computational diversity

Method 0: Unit-to-unit comparison using Z-scored cosine similarity (CS)

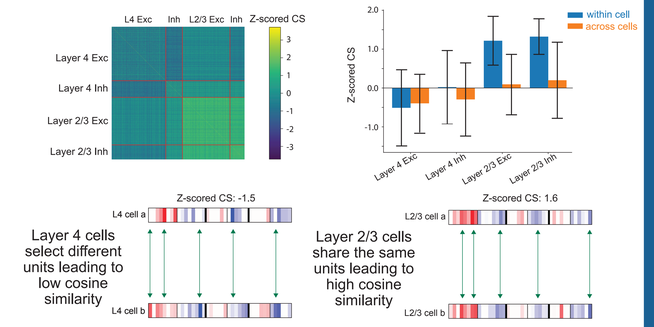

Method 1: Connectivity-based barcodes through within-layer sorting

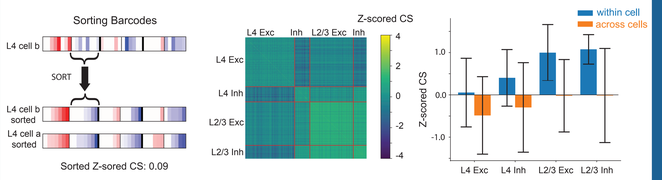

Method 2: Projecting into a functionally relevant subspace using clustering

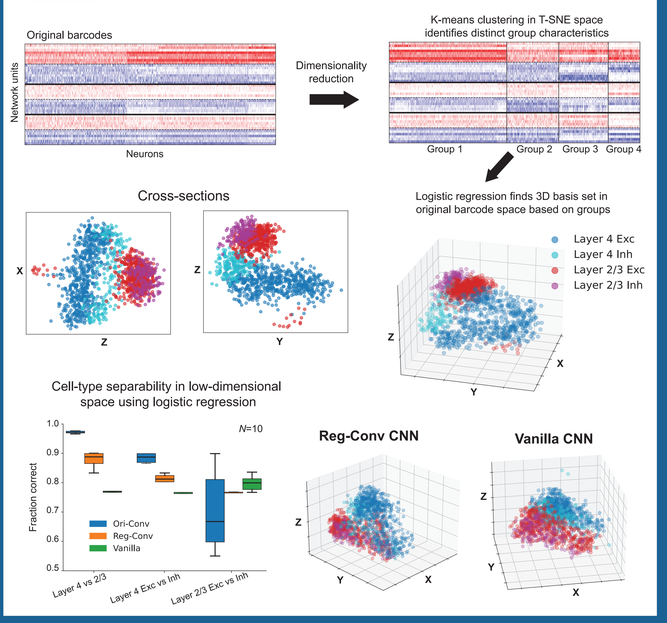

Conclusions

1. Computational barcodes describe neural function in common functional space, and capture computationally relevant distinctions between different parts of the cortical circuits
2. Biological constraints on the CNN leads to a more interpretable representations of V1 computations
3. Connectivity and a low-D "barcode space" demonstrates geometric relationships between neuronal computations
4. Distinct groups of computations found in (real) V1, and chromatic processing can potentially aid in circuit identification

Preliminary: color processing in V1

This approach was applied to data recorded in the Conway lab in macaque V1 using spatiotemporal chromatic stimuli (see Methods)

Using an LGN-bottleneck constrained in LMS space, the CNN inferred spatiotemporal-chromatic features resembling parvocellular (first 6) and magnocellular (last 2) units

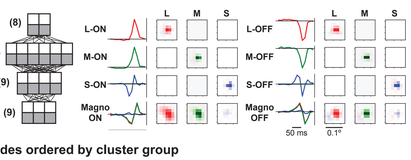

Barcodes ordered by cluster group

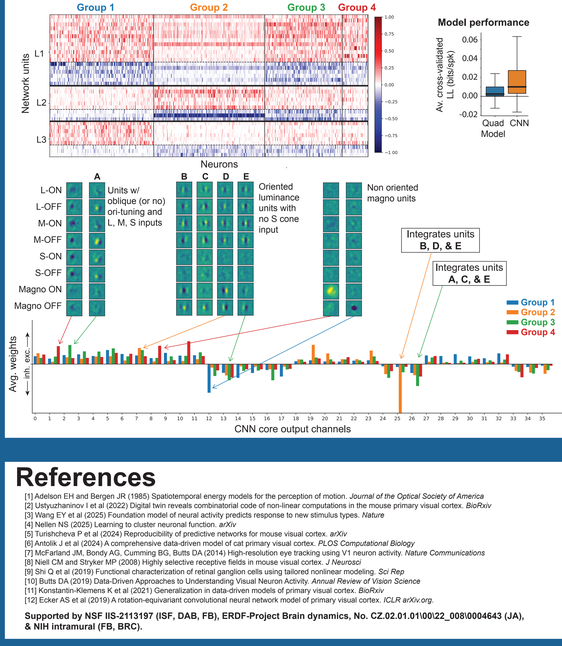

Methods

Simulated cat V1 data (Antolik et al. 2024 [6])

Data was generated from a large-scale spiking model of V1 with cell types and connectivity that constrained by known anatomy and able to reproduce classical and extra-classical V1 tuning properties. The simulation integrates differential equations and neurons are integrate-and-fire, with the simulation encompassing over 100,000 labeled neurons across 5° of visual field. For analysis, cells within 0.3° were selected, yielding 607 Layer 4 excitatory, 187 Layer 4 inhibitory, 535 Layer 2/3 excitatory, and 162 Layer 2/3 inhibitory units.

The resulting simulaed neural responses (spikes) were fit as if real recorded data, but the specific connectivity properties of each simulated neuron was known exactly, so could be used to test the ability of our approach to indentify the different computations carried out at different stages (layer, exc/inh).

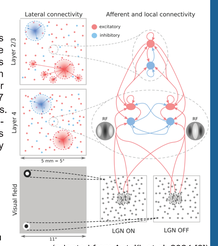

(adapted from Antolík et al. 2024 [6])

Macaque V1 recordings (Conway lab, NIH)

Recordings from macaque V1 were made using a Utah array, while the monkey passively fixated over 4-sec trials, using standard approaches [7]. We pooled data from five recordings, yielding 726 units (with 349 single units) that was used in our approach. Recordings were performed by Felix Bartsch and Bevil Conway.

Color Cloud Frame

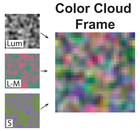

Cloud stimuli

In both stimulation and experiments, we presented cloud stimuli [8,9], which is 60 Hz spatiotemporal white noise spatially band-passed in the range of 6-30 cycles per degree to optimally drive V1 responses while maintaining a statistically stable but highly variable context to fit models of V1 responses. For macaque experiments, we used three independent clouds to cover DKL color space, in luminance, L-M, and S-dimensions. Note that such stimuli could be converted to an equivalent LMS (cone) space, which was done in preliminary analyses (in the far right). Stimuli were continuously adjusted for the eye position to represent the image on the retina. The five experiments used here represented between 40-60 minutes each of continuous data. Repeated stimuli were not possible because of eye movements.

Because the cat V1 simulation did not have color processing, we simulated response to simply luminance clouds, without any cone-opponent channels. The simulated data consisted of responses to 480,000 frames of the stimulus at 60 Hz resolution, split into training and validation, and 100,000 frames with 10 repeats for model performance testing (i.e., R^2).

Maximum a posteriori (MAP) estimation of CNN parameters [10]

CNNs of various configurations were fit to the neural data described using *PyTorch.* via using stochastic gradient descent (the AdamW optimizer) to maximize the regularization-penalized population Poisson log-likelihood (per spike), given by

$$LL_{pop} = \sum_i^{N_{neur}} \frac{1}{N_{spks}^{(i)}} \sum_t^T d_i(t)\{R_{obs}^{(i)}(t)\log_2 r_i(t) - r_i(t)\} - (\text{regularization penalties})$$

where $r_i(t)$ is the model predicted firing rate, and $d_i(t) = 1$ for all time points where there is recorded data for neuron i, and zero otherwise. CNN convolutional layers consisted of filters, batch-norm, and a ReLU, and followed by a final "readout" layer with a softplus activation function. The readout layer sampled from a single spatial (and orientation for the ori-conv model) of the outputs of the core in the network for each cell [11]. We constrained the readout weights to be positive, and a third of the units in each level were made to be "inhibitory" by multiplying their output by -1.

References

[1] Adelson EH and Bergen JR (1985) Spatiotemporal energy models for the perception of motion. *Journal of the Optical Society of America*
[2] Ustyuzhaninov I et al (2022) Digital twin reveals combinatorial code of non-linear computations in the mouse primary visual cortex. *BioRxiv*
[3] Wang EY et al (2025) Foundation model of neural activity predicts response to new stimulus types. *Nature*
[4] Nellen NS (2025) Learning to cluster neuronal function. *arXiv*
[5] Turishcheva P et al (2024) Reproducibility of predictive networks for mouse visual cortex. *arXiv*
[6] Antolik J et al (2024) A comprehensive data-driven model of cat primary visual cortex. *PLOS Computational Biology*
[7] McFarland JM, Bondy AG, Cumming BG, Butts DA (2014) High-resolution eye tracking using V1 neuron activity. *Nature Communications*
[8] Nieli CM and Stryker MP (2008) Highly selective receptive fields in mouse visual cortex. *J Neurosci*
[9] Shi Q et al (2019) Functional characterization of retinal ganglion cells using tailored nonlinear modeling. *Sci Rep*
[10] Butts DA (2019) Data-Driven Approaches to Understanding Visual Neuron Activity. *Annual Review of Vision Science*
[11] Konstantin-Klemens K et al (2021) Generalization in data-driven models of primary visual cortex. *BioRxiv*
[12] Ecker AS et al (2019) A rotation-equivariant convolutional neural network model of primary visual cortex. *ICLR arXiv.org.*

Supported by NSF IIS-2113197 (ISF, DAB, FB), ERDF-Project Brain dynamics, No. CZ.02.01.01\00\22_008\0004643 (JA), & NIH intramural (FB, BRC).